

## Fast detector of the ellipticity of infrared and terahertz radiation based on HgTe quantum well structures

S. N. Danilov, B. Wittmann, P. Olbrich, W. Eder, W. Prettl et al.

Citation: *J. Appl. Phys.* **105**, 013106 (2009); doi: 10.1063/1.3056393

View online: <http://dx.doi.org/10.1063/1.3056393>

View Table of Contents: <http://jap.aip.org/resource/1/JAPIAU/v105/i1>

Published by the [American Institute of Physics](#).

---

### Related Articles

Influence of laser lift-off on optical and structural properties of InGaN/GaN vertical blue light emitting diodes  
[AIP Advances 2, 022122 \(2012\)](#)

Vertical nonpolar growth templates for light emitting diodes formed with GaN nanosheets  
[Appl. Phys. Lett. 100, 033119 \(2012\)](#)

Irregular spectral position of E || c component of polarized photoluminescence from m-plane InGaN/GaN multiple quantum wells grown on LiAlO<sub>2</sub>  
[Appl. Phys. Lett. 99, 232114 \(2011\)](#)

Improvement in spontaneous emission rates for InGaN quantum wells on ternary InGaN substrate for light-emitting diodes  
[J. Appl. Phys. 110, 113110 \(2011\)](#)

Influence of high temperature AlN buffer on optical gain in AlGaIn/AlGaIn multiple quantum well structures  
[Appl. Phys. Lett. 99, 171912 \(2011\)](#)

---

### Additional information on J. Appl. Phys.

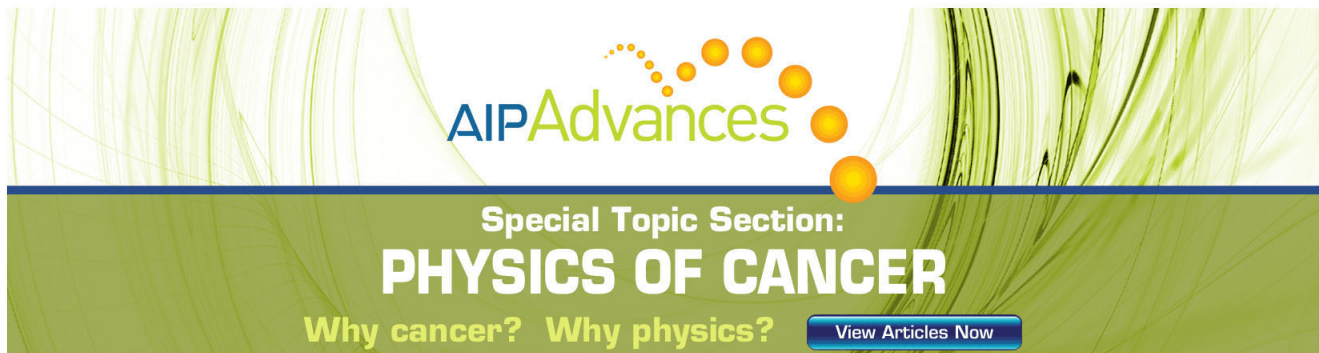
Journal Homepage: <http://jap.aip.org/>

Journal Information: [http://jap.aip.org/about/about\\_the\\_journal](http://jap.aip.org/about/about_the_journal)

Top downloads: [http://jap.aip.org/features/most\\_downloaded](http://jap.aip.org/features/most_downloaded)

Information for Authors: <http://jap.aip.org/authors>

## ADVERTISEMENT



The advertisement banner features a green background with abstract, flowing lines. At the top, the text "AIPAdvances" is displayed in a stylized font, with "AIP" in blue and "Advances" in green. Below this, the text "Special Topic Section:" is written in white, followed by "PHYSICS OF CANCER" in large, bold, white capital letters. At the bottom, the text "Why cancer? Why physics?" is written in yellow, and a blue button with the text "View Articles Now" is located on the right side.

# Fast detector of the ellipticity of infrared and terahertz radiation based on HgTe quantum well structures

S. N. Danilov,<sup>1</sup> B. Wittmann,<sup>1</sup> P. Olbrich,<sup>1</sup> W. Eder,<sup>1</sup> W. Prettl,<sup>1</sup> L. E. Golub,<sup>2</sup>  
E. V. Beregulin,<sup>2</sup> Z. D. Kvon,<sup>3</sup> N. N. Mikhailov,<sup>3</sup> S. A. Dvoretzky,<sup>3</sup> V. A. Shalygin,<sup>4</sup>  
N. Q. Vinh,<sup>5</sup> A. F. G. van der Meer,<sup>5</sup> B. Murdin,<sup>6</sup> and S. D. Ganichev<sup>1,a)</sup>

<sup>1</sup>*Terahertz Center, University of Regensburg, 93040 Regensburg, Germany*

<sup>2</sup>*A. F. Ioffe Physico-Technical Institute, Russian Academy of Sciences, 194021 St. Petersburg, Russia*

<sup>3</sup>*Institute of Semiconductor Physics, Russian Academy of Sciences, 630090 Novosibirsk, Russia*

<sup>4</sup>*St. Petersburg State Polytechnic University, 195251 St. Petersburg, Russia*

<sup>5</sup>*FOM Institute for Plasma Physics, "Rijnhuizen," P.O. Box 1207, NL-3430 BE Nieuwegein, The Netherlands*

<sup>6</sup>*University of Surrey, Guildford, Surrey GU2 7XH, United Kingdom*

(Received 15 October 2008; accepted 18 November 2008; published online 8 January 2009)

We report a fast, room temperature detection scheme for the polarization ellipticity of laser radiation, with a bandwidth that stretches from the infrared to the terahertz range. The device consists of two elements, one in front of the other, that detect the polarization ellipticity and the azimuthal angle of the ellipse. The elements, respectively, utilize the circular photogalvanic effect in a narrow gap semiconductor and the linear photogalvanic effect in a bulk piezoelectric semiconductor. For the former we characterized both a HgTe quantum well and bulk Te, and for the latter, bulk GaAs. In contrast with optical methods we propose is an easy to handle all-electric approach, which is demonstrated by applying a large number of different lasers from low power, continuous wave systems to high power, pulsed sources. © 2009 American Institute of Physics. [DOI: 10.1063/1.3056393]

## I. INTRODUCTION

Fast and easy recording of the state of polarization, i.e., measurements of the Stokes parameters of a radiation field, is of great importance for various applications in science and technology. In particular the ellipticity of transmitted, reflected, or scattered light may be used to analyze the optical anisotropy of a wide range of media. The established method for gaining information about the polarization state of light is the use of optical elements to determine optical path differences. Recently we presented a technique that allows *all-electric* room temperature detection of the state of polarization providing full characterization of laser beams at terahertz frequencies.<sup>1,2</sup> The operation of the detector system is based on photogalvanic effects in semiconductor quantum well (QW) structures of suitably low symmetry.<sup>3,4</sup> The detection principle has been demonstrated on doped GaAs and SiGe QWs at room temperature applying terahertz molecular lasers as radiation sources.<sup>1,2</sup> The time constant of photogalvanic currents is determined by the momentum relaxation time of free carriers, which is in the range of picoseconds at room temperature. This makes possible to measure the state of polarization of laser radiation with subnanosecond time resolution. Here we report a substantial improvement of the sensitivity of the method by about two orders of magnitude higher compared to those previously reported in GaAs QWs and on the extension of the detector's spectral range from terahertz to the midinfrared in a single device. To achieve these goals we studied photogalvanic effects in QWs prepared from the narrow gap semiconductor HgTe and also

analyzed bulk single-crystalline Te and GaAs. HgTe QWs are promising narrow gap materials characterized by high electron mobilities, low effective masses, an inverted band structure, large  $g$  factors, and spin-orbit splittings of subbands in the momentum space.<sup>5-9</sup> Because of these features low dimensional HgTe/CdHgTe structures hold a great potential for detection of terahertz radiation<sup>3,10-14</sup> and for the rapidly developing field of spintronics.<sup>15-17</sup> The most important property of the materials relevant for the detection of the radiation ellipticity is the magnitude of the circular photogalvanic effect (CPGE),<sup>1-3</sup> which gives access to the helicity of a radiation field. Therefore we focus our work on the study of the CPGE. We show that HgTe QWs can be used for all-electric detection of radiation ellipticity in a wide spectral range from far-infrared (terahertz radiation) to midinfrared wavelengths. The detection is demonstrated for various low power *cw* and high power *pulsed* laser systems. A large spectral range was covered by low-pressure *cw*, pulsed, and *Q*-switched CO<sub>2</sub> lasers and high-power pulsed transverse excited atmospheric (TEA) pressure CO<sub>2</sub> lasers, which are used directly in the infrared range or as pump sources for terahertz molecular lasers. In addition measurements were carried out with a free-electron laser making use of its tunability and short pulses.

## II. EXPERIMENTAL

The experiments were carried out on Cd<sub>0.7</sub>Hg<sub>0.3</sub>Te/HgTe/Cd<sub>0.7</sub>Hg<sub>0.3</sub>Te single QWs of 21 nm width. The structures were grown on GaAs substrates with surface orientation (013) by means of a modified molecular beam epitaxy method.<sup>18</sup> Samples with electron densities of

<sup>a)</sup>Electronic mail: sergey.ganichev@physik.uni-regensburg.de.

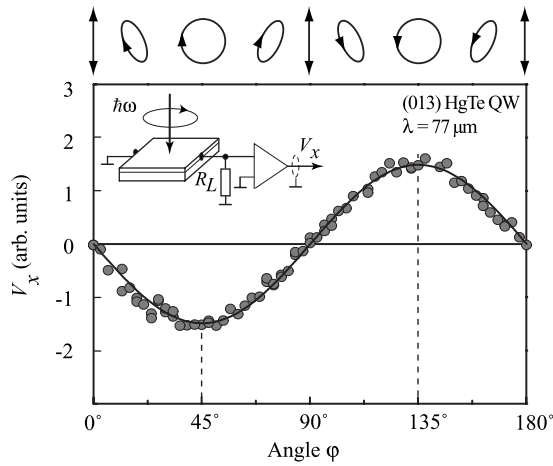


FIG. 1. Helicity dependence of the photoresponse normalized by the radiation power  $V_x/P$  in a (013)-grown HgTe QW at room temperature. The signals are obtained at  $\lambda = 77 \mu\text{m}$  applying pulsed radiation of  $\text{NH}_3$  terahertz laser. The full line is a fit after Eq. (1). The inset shows the experimental geometry. On top of the figure polarization ellipses corresponding to various phase angles  $\varphi$  are plotted viewing from the direction toward which the wave approaches.

$9 \times 10^{11} \text{ cm}^{-2}$  and mobility  $2.5 \times 10^4 \text{ cm}^2/\text{V s}$  are studied at room temperature. We used square shaped samples of  $5 \times 5 \text{ mm}^2$  size. Two pairs of contacts (along directions  $x$  and  $y$ ) were centered in the middle of cleaved edges parallel to the intersection of the (013) plane and cleaved edge face  $\{110\}$  (see the inset in Fig. 1). To demonstrate the detector operation in the midinfrared spectral range, we used a  $Q$ -switched  $\text{CO}_2$  laser covering the spectrum from  $9.2$  to  $10.8 \mu\text{m}$  with peak power  $P$  of about  $1 \text{ kW}$  and pulsed TEA- $\text{CO}_2$  laser generating single  $100 \text{ ns}$  pulses of power up to  $100 \text{ kW}$ .<sup>3</sup> Besides gas lasers we used the output from the free electron laser “FELIX” at FOM-Rijnhuizen in the Netherlands at wavelengths between  $5$  and  $17 \mu\text{m}$  and power about  $100 \text{ kW}$ .<sup>19</sup> Making use of the frequency tunability and short pulse duration of this laser, we obtain the spectral behavior of the detector responsivity and demonstrated its time resolution. The output pulses of light from FELIX were chosen to be  $\approx 3 \text{ ps}$  long, separated by  $40 \text{ ns}$ , in a train (or “macropulse”) of duration of  $7 \mu\text{s}$ . The macropulses had a repetition rate of  $5 \text{ Hz}$ . For optical excitation in the terahertz range we used a cw optically pumped  $\text{CH}_3\text{OH}$  laser with radiation wavelength of  $118 \mu\text{m}$  and power  $P$  of about  $10 \text{ mW}$  and high power pulsed optically pumped  $\text{NH}_3$ ,  $\text{D}_2\text{O}$ , and  $\text{CH}_3\text{F}$  lasers.<sup>3</sup> Several lines of the pulsed laser with power ranging from  $100 \text{ W}$  to  $100 \text{ kW}$  in the wavelength range between  $\lambda = 76$  and  $496 \mu\text{m}$  have been applied.

To vary the ellipticity of the laser beam we used  $\lambda/4$  plates made of  $x$ -cut crystalline quartz in the terahertz range and a Fresnel rhomb in the midinfrared. The light polarization was varied from linear to elliptical. Rotating the polarizer varies the helicity of the light,  $P_{\text{circ}} = \sin 2\varphi$ , from  $P_{\text{circ}} = -1$  (left-handed circular,  $\sigma_-$ ) to  $P_{\text{circ}} = +1$  (right-handed circular,  $\sigma_+$ ) where  $\varphi$  is the angle between the initial linear polarization and the optical axis ( $c$ -axis) of the polarizer. In Fig. 1 (top) the shape of the polarization ellipse and the handedness of the radiation are shown for various angles  $\varphi$ .

Photogalvanic effects applied here for radiation detec-

tion generate an electric current, which we measure in homogeneously irradiated unbiased samples. The current is converted into a signal voltage by load resistors. The signal voltages were picked up from the detector across a  $R_L = 50 \Omega$  load resistor for short radiation pulses. For cw irradiation we use a load resistance of  $1 \text{ M}\Omega$ , which is much higher than the sample resistance. For pulsed lasers the signals were fed into amplifiers with voltage amplification by a factor of 100 and a bandwidth of  $300 \text{ MHz}$  and were recorded by a digital broadband ( $1 \text{ GHz}$ ) oscilloscope. For time resolved measurements the signal was picked up directly from the sample without amplification. For detection of cw laser radiation we modulated our beam with a chopper at modulation frequency of  $225 \text{ Hz}$  and used a low-noise preamplifier (100 times voltage amplification) and a lock-in-amplifier for signal recording. We note that in this low modulation frequency case the high time resolution of the setup is not required.

### III. DETECTION OF THE HELICITY APPLYING HgTe QWs

With illumination of HgTe samples at normal incidence we detected in the in-plane  $x$ -direction a helicity dependent current signal. This is shown in Fig. 1 for a measurement at room temperature obtained at  $77 \mu\text{m}$  wavelength and power  $P \approx 10 \text{ kW}$  of a pulsed  $\text{NH}_3$  laser. Note that the measurement is dc coupled and no background subtraction has occurred. The signal changes direction if the circular polarization is switched from left- to right-handed and vice versa. The dependence on the helicity  $P_{\text{circ}}$  and in particular the change in sign demonstrate that the observed current  $j_x$  is due to the CPGE.<sup>3</sup> The voltage signal resulting from the photocurrent  $V_x \propto j_x$  is well described by

$$V_x^{\text{HgTe}} = S(\omega)P \cdot P_{\text{circ}}, \quad (1)$$

where  $S(\omega)$  denotes the strength of CPGE at radiation frequency  $\omega$  and, consequently, the sensitivity of this detector unit. The photogalvanic current is described by the phenomenological theory. It can be written as a function of the electric component of the radiation field  $\mathbf{E}$  and the propagation direction  $\hat{\mathbf{e}}$  in the following form:<sup>4,17</sup>

$$j_\lambda = \sum_\rho \gamma_{\lambda\rho} \hat{e}_\rho P_{\text{circ}} |E|^2 + \sum_{\mu,\nu} \chi_{\lambda\mu\nu} (E_\mu E_\nu^* + E_\mu^* E_\nu), \quad (2)$$

where the first term on the right hand side being proportional to the helicity or circular polarization degree  $P_{\text{circ}}$  of the radiation represents the CPGE, while the second term corresponds to the linear photogalvanic effect (LPGE),<sup>3</sup> which may be superimposed to the CPGE. The indices  $\lambda$ ,  $\rho$ ,  $\mu$ , and  $\nu$  run over the coordinate axes  $x$ ,  $y$ , and  $z$ . The second rank pseudotensor  $\gamma_{\lambda\rho}$  and the third rank tensor  $\chi_{\lambda\mu\nu}$  symmetric in the last two indices are material parameters. The (013)-oriented QWs belong to the trivial point group  $C_1$  lacking any symmetry operation except the identity. Hence symmetry does not impose any restriction on the relation between irradiation and photocurrent. All components of the tensor  $\chi_{\lambda\mu\nu}$  and the pseudotensor  $\gamma_{\lambda\rho}$  may be different from zero. Equa-



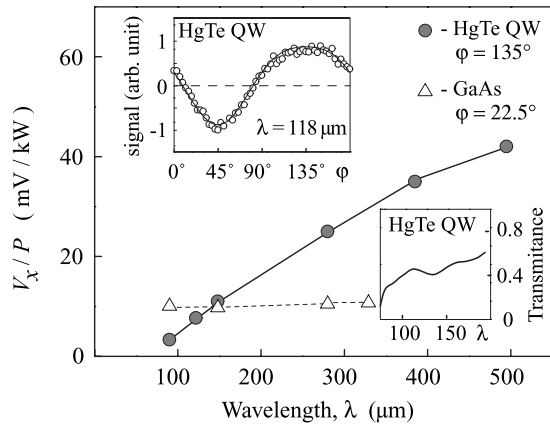


FIG. 2. CPGE spectrum of HgTe QW (full circles) in the terahertz-range normalized by power incident on the sample for circularly polarized radiation ( $\varphi=135^\circ$ ). Top inset shows the helicity dependence obtained in HgTe QW applying radiation of a cw CH<sub>3</sub>OH laser at  $\lambda=118\ \mu\text{m}$ . Full line in the inset is the fit after Eq. (3). Bottom inset shows transmittance spectrum obtained by FTIR spectroscopy. Triangles show the spectrum of bulk GaAs sample in response to the elliptically polarized radiation. The data are given for angles  $\varphi=22.5^\circ$  corresponding to the maximum of the voltage signal.

tion (2) yields for normal incidence of the radiation the angle  $\varphi$  dependence of the photosignal  $V_x \propto j_x$ ,

$$V_x/P = S(\omega)\sin 2\varphi + b(\omega)\sin 4\varphi + c(\omega)\cos 4\varphi + d(\omega), \quad (3)$$

where  $S(\omega)$ ,  $b(\omega)$ ,  $c(\omega)$ , and  $d(\omega)$  can be consistently expressed by components of the tensors  $\gamma_{\lambda\rho}$  and  $\chi_{\lambda\mu\nu}$  defined in Eq. (2).<sup>20</sup> While at most wavelengths we found that the first term in Eq. (3) dominates (see Fig. 1), at some wavelengths we also find a small polarization independent current offset and a slight distortion of the sine-shape of the  $V_x$  versus  $\varphi$  curve. This deviation from the  $\sin 2\varphi$  behavior is demonstrated in the inset in Fig. 2 for  $118\ \mu\text{m}$  wavelength of the cw CH<sub>3</sub>OH laser. The solid line in this inset is calculated after Eq. (3) yielding a good agreement to the experiment. Note, however, that for a technical application as an ellipticity detector described here, it is desirable to have samples with dominating CPGE term being simply proportional to  $P_{\text{circ}}$  like the photoresponse in Fig. 1. For all wavelengths this goal could be achieved by using technologically available (112)-grown samples.<sup>6</sup> The reason is the higher symmetry of such structures. In (013)-oriented samples investigated in our work the CPGE current can have arbitrary direction and, in fact, the projection of the current on the connecting line between the contacts is measured. Furthermore three LPGE current contributions are allowed due to the low symmetry of the samples. In contrast, in (112)-grown structures the current direction for normal incidence is bound to the  $[1\bar{1}0]$ -crystallographic direction. This is because such samples belong to the  $C_s$  point group forcing the CPGE current to a direction normal to the mirror reflection plane. This feature makes the preparation of samples with dominating CPGE for all wavelengths possible. Picking up the signal from the  $[1\bar{1}0]$ -direction should increase the sensitivity and smoothen the spectral dependence.

In Figs. 2 and 3 the spectral dependence of the CPGE is shown for the terahertz and infrared ranges, respectively. The

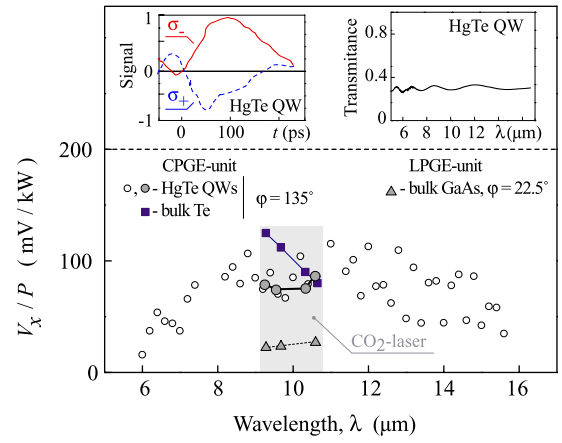


FIG. 3. (Color online) CPGE spectrum of HgTe QW and Te bulk crystal obtained in response to the midinfrared circular polarized radiation and normalized by power incident on the sample for circularly polarized radiation. The data are obtained for angles  $\varphi=135^\circ$  applying  $Q$ -switched CO<sub>2</sub> laser (full circles) and free electron laser FELIX (open circles). The data of Te are plotted by squares. Triangles represent spectral response of the LPGE bulk GaAs unit obtained by pulsed TEA-CO<sub>2</sub> laser radiation. The data are given for angles  $\varphi=22.5^\circ$  corresponding to the maximum of the voltage signal. The shadow area indicates the spectral range of a CO<sub>2</sub> laser. Left and right insets show the CPGE temporal response of HgTe QWs to subpicosecond infrared pulses of FELIX ( $\lambda=9\ \mu\text{m}$ ) and the transmittance spectra obtained by FTIR spectroscopy, respectively.

measurements are carried out at room temperature at normal incidence of radiation and for circularly polarized radiation ( $\varphi=135^\circ$ ) where the CPGE signal is maximal. In the terahertz range molecular lasers were applied, while the measurements in the infrared range were performed using FELIX (open circles in Fig. 3) and a  $Q$ -switched CO<sub>2</sub> laser (full circles in Fig. 3). In the infrared range CPGE in HgTe QWs does not show much dispersion for  $\lambda$  between 8 and  $14\ \mu\text{m}$ , while in the terahertz range the photocurrent rises significantly with the increasing wavelength. The spectral behavior of the signal is mainly caused by the mechanism involved in the radiation absorption, interband in the midinfrared range, and Drude-like in the terahertz range. The sensitivity in the midinfrared range being of the order of 80 mV/kW is comparable with that of photon drag detectors widely applied for detection of infrared laser radiation.<sup>3,21,22</sup> Comparing sensitivities of HgTe QW and GaAs QW devices in the terahertz range, we obtain that a detector element made of one single HgTe QW ( $S=10\ \text{mV/kW}$  for  $\lambda=148\ \mu\text{m}$ ) has about 100 times higher sensitivity per QW than devices based on GaAs QWs.<sup>23</sup> The sensitivity of HgTe QW based devices can be further improved simply by using a larger number of QWs.

To determine the time resolution of our device we used 3 ps pulses of FELIX. The left inset in Fig. 3 shows that the response time is at most 100 ps. We attribute the observed time constant to the bandwidth of our electronic setup. A fast response is typical for photogalvanics where the signal decay time is determined by the momentum relaxation time<sup>3,17</sup> being in our samples of the order of 0.3 ps at room temperature. As a large dynamic range is important for detection of laser radiation, we investigated the dependence of the sensitivity of the detection system on the radiation intensity applying cw and high-power pulsed radiation. We observed that

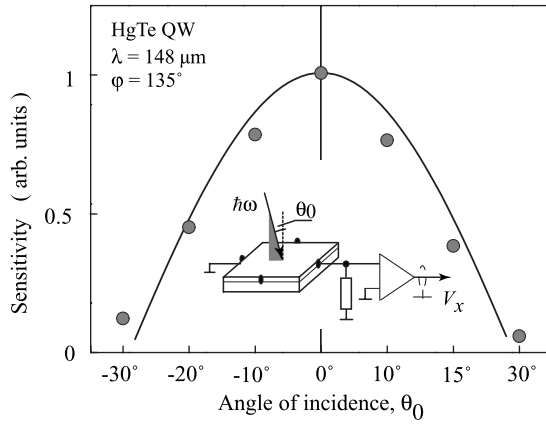


FIG. 4. Sensitivity of the (013)-oriented HgTe QW CPGE-detector unit as a function of the angle of incidence for circularly polarized radiation. The data are shown for the rotation of the angle of incidence in the  $(xz)$ -plane. Full line shows the fit to the data to the phenomenological theory taken into account besides CPGE, an additional contribution of the circular photon drag effect (Ref. 25).

the ellipticity detector at homogeneous irradiation of the whole sample remains linear up to  $2 \text{ MW/cm}^2$  over more than nine orders of magnitude.

In a further experiment we checked the variation in the sensitivity due to a deviation from normal incidence of radiation. Measurements at oblique incidence demonstrate that the CPGE current attains maximum at normal incidence. This is shown in Fig. 4 for angles of incidence  $\theta_0$  in the range  $\pm 30^\circ$  at a wavelength  $\lambda = 148 \text{ } \mu\text{m}$  and for circularly polarized light. We find that the sensitivity is reduced at a deviation from normal incidence. This behavior follows from Eq. (2) yielding  $j \propto t_p t_s \cos \theta$ , where  $t_p$  and  $t_s$  are the Fresnel transmission coefficients for  $s$ - and  $p$ -polarized light, and  $\theta$  is the refraction angle given by  $\sin \theta = \sin \theta_0 / n_\omega$  where  $n_\omega$  is the refraction index.<sup>24</sup> Experimentally, however, we observed that in our samples the photocurrent drops more strongly with increasing  $\theta_0$  than expected from Fresnel's formula. We attribute this effect to a superposition of CPGE with the circular photon drag effect<sup>25</sup> at oblique incidence. Because both effects are proportional to  $P_{\text{circ}}$  and have the same temporal kinetic, this superposition does not compromise the detector's functionality.

#### IV. DETECTION OF THE ELLIPSE'S AZIMUTH ANGLE WITH BULK GaAs

To obtain all Stokes parameters besides the CPGE that provides an information on the radiation helicity, an additional detector element for determination of the ellipse azimuth is needed.<sup>1</sup> In our previous work aimed at the detection of terahertz radiation we used for this purpose the linear photogalvanic effect in SiGe QWs. The LPGE in SiGe structures is also detected in the midinfrared range.<sup>26</sup> However, the signal is rather small and the response is obtained only at wavelength about  $10 \text{ } \mu\text{m}$  under resonant intersubband transitions. To search for other materials, with the aim to increase the sensitivity and to extend the spectral range of the detector, we analyze here the LPGE in bulk GaAs crystals. Bulk GaAs crystals belong to  $T_d$  point group symmetry.

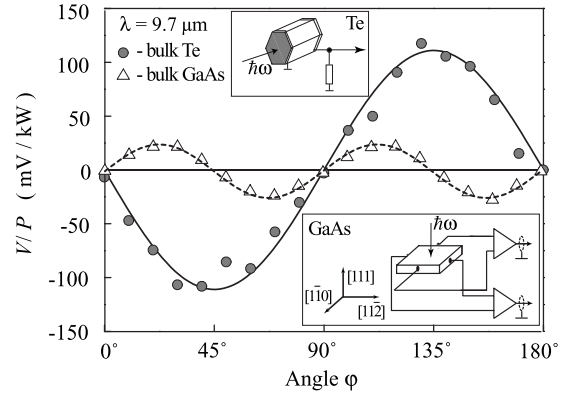


FIG. 5. Helicity dependence of the photoresponse normalized by the radiation power  $V/P$  in bulk Te (circles) and bulk GaAs (triangles) samples at room temperature. The signals are obtained at  $\lambda = 9.7 \text{ } \mu\text{m}$  applying pulsed TEA  $\text{CO}_2$  laser radiation. Full and dashed lines are fits after  $V_z/P \propto \sin 2\varphi$  and  $V_{[110]}/P \propto \sin 4\varphi$  for Te and GaAs, respectively. Insets show the experimental geometry for both samples. In the GaAs-detector unit the signal of each contact pair is fed into a differential amplifier floating against ground.

While the CPGE in materials of this symmetry is forbidden, a LPGE current can be generated applying linearly or elliptically polarized radiation.

We prepared (111)-oriented  $p$ -type GaAs samples of  $5 \times 5 \times 2 \text{ mm}^3$  sizes with a contact pair along the  $x \parallel [1\bar{1}0]$  and  $y \parallel [11\bar{2}]$  axes as sketched in Fig. 5. We used materials with free hole densities of about  $2.3 \times 10^{16} \text{ cm}^{-3}$  like it previously been used for detection of the plane of polarization of linearly polarized radiation.<sup>27</sup> In our measurements we aligned the  $[1\bar{1}0]$  side of the sample parallel to the light polarization vector of the laser beam. The current of each contact pair is fed into a differential amplifier floating against ground.

According to Eq. (2) irradiation with polarized radiation propagating in the  $[111]$  crystallographic direction yield transverse signals given by

$$\begin{aligned} \frac{V_{[11\bar{2}]} }{P} &= C(\omega) \frac{(|E_x|^2 - |E_y|^2)}{|E|^2}, \\ \frac{V_{[1\bar{1}0]} }{P} &= C(\omega) \frac{(E_x E_y^* + E_y E_x^*)}{|E|^2}, \end{aligned} \quad (4)$$

where  $C(\omega)$  is a constant factor being proportional to the only one nonzero component of the third rank tensor  $\chi$ .<sup>24</sup> In our experimental setup where the radiation ellipticity is varied by the rotation of the quarter-wave plate by an angle  $\varphi$ ,  $(|E_x|^2 - |E_y|^2)/|E|^2 = (1 + \cos 4\varphi)/2$ , and  $(E_x E_y^* + E_y E_x^*)/|E|^2 = \sin 4\varphi/2$ . Applying infrared radiation we clearly detected both dependences of the photosignal. Figure 5 shows the angle  $\varphi$  dependence of  $V_{[1\bar{1}0]}/P$  obtained applying radiation at  $\lambda = 9.7 \text{ } \mu\text{m}$ .

From the angle  $\varphi$  dependence we obtain the LPGE constant  $C(\omega)$ , which determines the detector element sensitivity providing the calibration of the device. Figure 3 shows the spectral behavior of the constant  $C(\omega)$  at infrared wavelengths obtained by the  $Q$ -switched  $\text{CO}_2$  laser. The sensitivity of the order of  $20 \text{ mV/kW}$  is measured for the angle  $\varphi = 22.5^\circ$  at which signal achieves its maximum value. This

value is comparable to that of the HgTe QW CPGE-detector unit. We also obtained a considerable signal in the terahertz range characterized by the same angle  $\varphi$  dependences. Here the sensitivity at 148  $\mu\text{m}$  is also comparable to that of the HgTe QW CPGE-detector unit and is about 20 times higher than that measured previously in SiGe QWs.<sup>2</sup>

To obtain the Stokes parameters of a radiation field the signals from HgTe QW and bulk GaAs must be measured simultaneously. In the work on a terahertz ellipticity detector we simply stacked the CPGE- and the LPGE-detector units. This arrangement is only possible if the first of the two elements is practically transparent to the incident radiation. Therefore we carried out Fourier transform infrared (FTIR) measurements of the transmission of HgTe QW. These data are shown in the insets in Figs. 2 and 3. The essential result is that the sample is almost transparent and can be used in a stacked configuration. The transmittance in the whole spectral range is about 30%–40%, which just corresponds to the reflectivity of the sample. The oscillations in the spectrum are due to interference in the plane-parallel transparent semiconductor slab. The magnitude of the reflection can be reduced by antireflection coatings improving the sensitivity of the detector system.

## V. STOKES PARAMETERS

From the signals obtained by the CPGE-detector unit (HgTe QW) and by the LPGE-unit (bulk GaAs), it follows that simultaneous measurements of two signals allow one the determination of the Stokes parameters, which completely characterize the state of polarization of the radiation field. The Stokes parameters defined according to Ref. 28 are directly measured in our detector units yielding

$$\begin{aligned} s_0 &= |E|^2, \\ \frac{s_1}{s_0} &= \frac{|E_x|^2 - |E_y|^2}{|E|^2} = \frac{V_{[11\bar{2}]}^{\text{GaAs}}}{PC(\omega)}, \\ \frac{s_2}{s_0} &= \frac{E_x E_y^* + E_y E_x^*}{|E|^2} = \frac{V_{[1\bar{1}0]}^{\text{GaAs}}}{PC(\omega)}, \\ \frac{s_3}{s_0} &= \frac{i(E_y E_x^* - E_x E_y^*)}{|E|^2} = P_{\text{circ}} = \frac{V_x^{\text{HgTe}}}{PS(\omega)}, \end{aligned} \quad (5)$$

where the parameter  $s_0 \propto P$  does not contain information about the polarization state and determines the radiation intensity.

## VI. CPGE UNIT BASED ON BULK Te

Finally we investigated CPGE in another narrow band semiconductor—bulk Te—with respect to its applicability in an ellipticity detector and compare the results with the data on HgTe QW structures. In fact bulk Te was the first material in which the CPGE was detected.<sup>29</sup> Single crystal Te belongs to the point group  $D_3$  where second rank pseudotensors are diagonal in a coordinate system with  $z$  along the trigonal crystallographic axis. This axis is also the growth direction

of bulk crystals. The macroscopic shape of Te is hexagonal. Thus, irradiating a sample along  $z$  direction generates a longitudinal current along this axis. Equation (2) yields for the photosignal  $V_z \propto j_z$  in Te (Ref. 30)

$$V_z/P = \tilde{S}(\omega)P_{\text{circ}}. \quad (6)$$

In order to measure this current we prepared two contacts around circumferences of hexagonal prism shaped specimens, see inset in Fig. 5. We used  $p$ -doped tellurium crystals, which at room temperature have the hole concentration of about  $3.5 \times 10^{16} \text{ cm}^{-3}$ . The samples were of 11.5 mm long and had a cross section of  $\approx 20 \text{ mm}^2$ . Illuminating the crystal along the  $z$  axis by midinfrared radiation we detected a polarization dependent signal reversing polarity upon switching the radiation helicity (see Fig. 5). In our experimental setup the radiation helicity is varied by the rotation of the quarter-wave plate by an angle  $\varphi$  according to  $P_{\text{circ}} = \sin 2\varphi$ . The signal  $V_z$  is well described by this dependence. The possible contribution of the longitudinal photon drag effect is vanishingly small in our samples at room temperature in agreement with Ref. 29. Figure 3 shows the spectral behavior of the sensitivity of the Te sample obtained for circularly polarized radiation. Our investigations demonstrate that in this material the sensitivity in the midinfrared is about three times higher than that observed for a HgTe single QW (Fig. 3). The data prove that bulk Te can be used as CPGE detector unit in the midinfrared. However, application of multiple HgTe QWs for which the sensitivity scales linearly with the number of QWs should provide a sensitivity substantially higher than that of Te making HgTe QWs preferable for ellipticity detection. In the terahertz range we did not find a CPGE signal in Te even when applying the highest available radiation power.

## VII. CONCLUSION

We demonstrated that the application of narrow gap low dimensional HgTe structures allows all-electric detection of the Stokes parameters of elliptically polarized radiation from the midinfrared to the terahertz range. The sensitivity and linearity of the detection system developed here have been found to be sufficient to characterize the polarization of laser radiation from low-power cw-lasers to high-power laser pulses. The short relaxation time of free carriers in semiconductors at room temperature makes it possible to detect subnanosecond laser pulses demonstrated with the free-electron-laser FELIX. Finally we note that a further increase in the sensitivity may be obtained by using multiple QWs and technologically available (112)-grown samples.

## ACKNOWLEDGMENTS

We thank S. A. Tarasenko, E. L. Ivchenko, and V. V. Bel'kov for useful discussions. The financial support of the DFG and RFBR is gratefully acknowledged. The work of L.E.G. is also supported by “Dynasty” Foundation—ICFPM and President grant for young scientists.

<sup>1</sup>S. D. Ganichev, J. Kiermaier, W. Weber, S. N. Danilov, D. Schuh, Ch. Gerl, W. Wegscheider, D. Bougeard, G. Abstreiter, and W. Prettl, *Appl.*

- Phys. Lett.* **91**, 091101 (2007).
- <sup>2</sup>S. D. Ganichev, W. Weber, J. Kiermaier, S. N. Danilov, D. Schuh, W. Wegscheider, Ch. Gerl, D. Bougeard, G. Abstreiter, and W. Prettl, *J. Appl. Phys.* **103**, 114504 (2008).
- <sup>3</sup>S. D. Ganichev and W. Prettl, *Intense Terahertz Excitation of Semiconductors* (Oxford University Press, Oxford, 2006).
- <sup>4</sup>E. L. Ivchenko, *Optical Spectroscopy of Semiconductor Nanostructures* (Alpha Science International, Harrow, United Kingdom, 2005).
- <sup>5</sup>A. Pfeuffer-Jeschke, F. Goschenhofer, S. J. Cheng, V. Latussek, J. Gerschütz, C. R. Becker, R. R. Gerhardts, and G. Landwehr, *Physica B* **256**, 486 (1998).
- <sup>6</sup>X. C. Zhang, A. Pfeuffer-Jeschke, K. Ortner, V. Hock, H. Buhmann, C. R. Becker, and G. Landwehr, *Phys. Rev. B* **63**, 245305 (2001).
- <sup>7</sup>X. C. Zhang, K. Ortner, A. Pfeuffer-Jeschke, C. R. Becker, and G. Landwehr, *Phys. Rev. B* **69**, 115340 (2004).
- <sup>8</sup>Y. S. Gui, C. R. Becker, N. Dai, J. Liu, Z. J. Qiu, E. G. Novik, M. Schäfer, X. Z. Shu, J. H. Chu, H. Buhmann, and L. W. Molenkamp, *Phys. Rev. B* **70**, 115328 (2004).
- <sup>9</sup>Z. D. Kvon, S. N. Danilov, N. N. Mikhailov, S. A. Dvoretzky, and S. D. Ganichev, *Physica E (Amsterdam)* **40**, 1885 (2008).
- <sup>10</sup>K. Sakai, *Terahertz Optoelectronics* (Springer, Berlin, 2005).
- <sup>11</sup>*Terahertz Frequency Detection and Identification of Materials and Objects*, edited by R. E. Miles, X.-C. Zhang, H. Eisele, and A. Krotkus (Springer, Berlin, 2007).
- <sup>12</sup>*Terahertz Science and Technology for Military and Security Applications*, edited by D. L. Woolard, J. O. Jensen, and R. J. Hwu (World Scientific, Singapore, 2007).
- <sup>13</sup>T. Edwards, *Gigahertz and Terahertz Technologies for Broadband Communications (Satellite Communications)* (Artech House, Boston, 2000).
- <sup>14</sup>*Electronic Devices and Advanced Systems Technology, Terahertz Sensing Technology Vol. 1*, edited by D. L. Woolard, W. R. Loerop, and M. Shur (World Scientific, Singapore, 2003).
- <sup>15</sup>*Semiconductor Spintronics and Quantum Computation*, edited by, D. D. Awschalom, D. Loss, and N. Samarth, Nanoscience and Technology, edited by K. von Klitzing, H. Sakaki, and R. Wiesendanger (Springer, Berlin, 2002).
- <sup>16</sup>I. Zutic, J. Fabian, and S. Das Sarma, *Rev. Mod. Phys.* **76**, 323 (2004).
- <sup>17</sup>*Spin Physics in Semiconductors*, edited by M. I. Dyakonov, Springer Series in Solid State Sciences, edited by M. Cardona, P. Fulde, K. von Klitzing, R. Merlin, H.-J. Queisser, H. Störmer (Springer, Berlin, 2008).
- <sup>18</sup>V. S. Varavin, V. V. Vasiliev, S. A. Dvoretzky, N. N. Mikhailov, V. N. Ovsyuk, Y. G. Sidorov, A. O. Suslyakov, M. V. Yakushev, and A. L. Aseev, *Proc. SPIE* **5136**, 381 (2003).
- <sup>19</sup>G. M. H. Knippels, X. Yan, A. M. MacLeod, W. A. Gillespie, M. Yasumoto, D. Oepts, and A. F. G. van der Meer, *Phys. Rev. Lett.* **83**, 1578 (1999).
- <sup>20</sup>B. Wittmann, S. N. Danilov, Z. D. Kvon, N. N. Mikhailov, S. A. Dvoretzky, R. Ravash, W. Prettl, and S. D. Ganichev, arXiv:0708.2169v1.
- <sup>21</sup>I. D. Yaroshetskii and S. M. Ryvkin, in *The Photon Drag of Electrons in Semiconductors*, Problems of Modern Physics, edited by V. M. Tuchkevich and V. Ya. Frenkel (Nauka, Leningrad, 1980), pp. 173–185 (in Russian) [English translation: *Semiconductor Physics*, edited by V. M. Tuchkevich and V. Ya. Frenkel (Consultants Bureau, New York, 1986) pp. 249–263].
- <sup>22</sup>A. F. Gibson and M. F. Kimmitt, in *Photon Drag Detection, Infrared and Millimeter Waves Vol. 3*, edited by K. J. Button (Academic, New York, 1980), pp. 181–217.
- <sup>23</sup>We note that in Ref. 2 applying GaAs structures made of thirty QWs we observed  $\approx 3$  mV/kW at  $\lambda = 148 \mu\text{m}$  corresponding to 0.1 mV/kW for a single QW.
- <sup>24</sup>E. L. Ivchenko and G. E. Pikus, *Superlattices and Other Heterostructures. Symmetry and Optical Phenomena* (Springer, Berlin, 1997).
- <sup>25</sup>V. A. Shalygin, H. Diehl, Ch. Hoffmann, S. N. Danilov, T. Herrle, S. A. Tarasenko, D. Schuh, Ch. Gerl, W. Wegscheider, W. Prettl, and S. D. Ganichev, *JETP Lett.* **84**, 570 (2007).
- <sup>26</sup>S. D. Ganichev, U. Rössler, W. Prettl, E. L. Ivchenko, V. V. Bel'kov, R. Neumann, K. Brunner, and G. Abstreiter, *Phys. Rev. B* **66**, 075328 (2002).
- <sup>27</sup>A. V. Andrianov, E. V. Beregulin, S. D. Ganichev, K. Yu. Gloukh, and I. D. Yaroshetskii, *Pis'ma Zh. Tekh. Fiz.* **14**, 1326 (1988); *Sov. Tech. Phys. Lett.* **14**, 580 (1988).
- <sup>28</sup>M. Born and E. Wolf, *Principles of Optics* (Pergamon Press, Oxford, 1964).
- <sup>29</sup>V. M. Asnin, A. A. Bakun, A. M. Danishevskii, E. L. Ivchenko, G. E. Pikus, and A. A. Rogachev, *Pis'ma Zh. Eksp. Teor. Fiz.* **28**, 80 (1978); *JETP Lett.* **28**, 74 (1978).
- <sup>30</sup>E. L. Ivchenko and G. E. Pikus, *Pis'ma Zh. Eksp. Teor. Fiz.* **27**, 640 (1978); *JETP Lett.* **27**, 604 (1978).